

## Refined solution structure of the DNA-binding domain of GAL4 and use of $^3J(^{113}\text{Cd},^1\text{H})$ in structure determination

James D. Baleja\*, Venkataraman Thanabal\*\* and Gerhard Wagner

Department of Biological Chemistry and Molecular Pharmacology, Harvard Medical School, Boston, MA 02115, U.S.A.

Received 27 August 1997

Accepted 15 October 1997

Keywords: GAL4; Cadmium; Coupling constant; Karplus relationship

### Summary

We have refined the solution structure of cadmium-bound GAL4 and present its  $^{15}\text{N}$  and  $^1\text{H}$  NMR assignments. The root-mean-square (rms) deviation to the average structure was  $0.4 \pm 0.05$  Å for backbone atoms, and  $0.9 \pm 0.1$  Å for all heavy atoms. The three-bond heteronuclear  $^3J(^{113}\text{Cd},^1\text{H})$  coupling constants were found to disobey a Karplus-type relationship, which was attributable to the unusual constraints imposed by the bimetal–thiolate cluster in GAL4. We conclude that the structural parameters that correlate to  $^3J(^{113}\text{Cd},^1\text{H})$  are complex.

The GAL4 protein activates transcription of the genes required for galactose utilization in *Saccharomyces cerevisiae* (Johnston, 1987). The N-terminal portion (residues 1–65) contains the amino acid residues responsible for DNA recognition and binding. The core of the DNA-binding domain contains a Cys-X<sub>2</sub>-Cys-X<sub>6</sub>-Cys-X<sub>6</sub>-Cys-X<sub>2</sub>-Cys-X<sub>6</sub>-Cys motif in which the six cysteines coordinate two zinc ions, forming a bimetal–thiolate cluster (Fig. 1) (Pan and Coleman, 1989,1990; Povey et al., 1990; Gardner et al., 1991; Baleja et al., 1992; Kraulis et al., 1992; Marmorstein et al., 1992; Shirakawa et al., 1993). The structure of the cadmium form of the protein has been determined by NMR (Baleja et al., 1992) and, in complex with DNA, by X-ray crystallography (Marmorstein et al., 1992). Here we report a refined solution structure of cadmium-bound GAL4 and its  $^{15}\text{N}$  and  $^1\text{H}$  NMR assignments. The three-bond  $^3J(^{113}\text{Cd},^1\text{H})$  coupling constant is considered for measuring torsion angles in cadmium-substituted proteins (Zerbe et al., 1994).

The DNA-binding domain containing the N-terminal 65 amino acid residues of GAL4 was prepared as described previously (Mau et al., 1992). The NMR sample contained 1.5 mM of Cd<sub>2</sub>(II)-GAL4 protein, an additional 10 μM

CdCl<sub>2</sub>, 0.1 M NaCl, 0.05% NaN<sub>3</sub>, 20 mM sodium phosphate, pH 7.18 (direct meter reading) at 25 °C.

Spectra were collected on a Bruker AMX-500 spectrometer with a proton frequency of 500.14 MHz as previously described (Baleja et al., 1992). The carrier frequency in the proton channel was set on the water resonance, which was suppressed using presaturation. A three-dimensional  $^{15}\text{N}$ -edited NOESY-HSQC spectrum was taken with a  $^1\text{H}$  spectral width of 8065 Hz, a  $^{15}\text{N}$  spectral width of 2941 Hz, a mixing time of 100 ms, 256 real t<sub>1</sub> points, 44 real t<sub>2</sub> ( $^{15}\text{N}$ ) points, and 1024 complex t<sub>3</sub> points (Mau et al., 1992). Spectra were processed with squared sine bells shifted by 35° in t<sub>3</sub> and 60° in t<sub>1</sub> and t<sub>2</sub>, using the FELIX NMR processing program. The final zero-filled matrix was 512 × 64 × 2048 points. Previous studies have shown that only residues 10–40 are structured into a recognition module, thus accounting for poor NOE intensity for residues outside the cluster (Gardner et al., 1991; Baleja et al., 1992; Kraulis et al., 1992; Shirakawa et al., 1993; Lefèvre et al., 1996). Accordingly, only residues 6 through 43 show appreciable intensity in the 3D spectrum and only these residues are discussed further.

Resonance assignments began with the identification of

\*To whom correspondence should be addressed at: Department of Biochemistry, Tufts University School of Medicine, 136 Harrison Avenue, Boston, MA 02111, U.S.A.

\*\*Present address: Parke-Davis Pharmaceutical Research, Division of Warner Lambert Company, 2800 Plymouth Road, Ann Arbor, MI 48105, U.S.A.

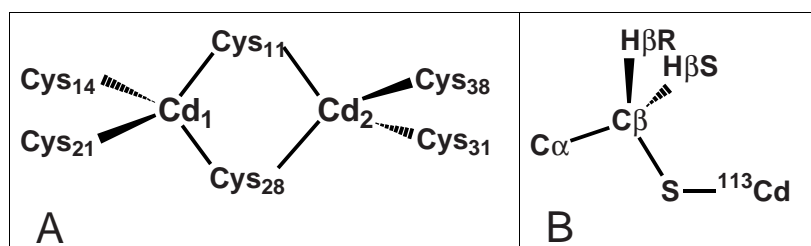


Fig. 1. Liganding of divalent cations by the bimetal thiolate cluster in the DNA-binding domain of GAL4. (A) The two central metal ions are ligated by six cysteine residues, with Cys<sup>11</sup> and Cys<sup>28</sup> forming a bridge between the cadmium ions. Cd<sub>1</sub> resonates at 669 ppm, whereas Cd<sub>2</sub> resonates at 707 ppm (Pan and Coleman, 1990). (B) Liganding of cadmium by a cysteine residue. In <sup>113</sup>Cd-substituted proteins, a three-bond (vicinal) coupling constant is observable between the β protons and cadmium.

TABLE 1  
<sup>1</sup>H AND <sup>15</sup>N NMR RESONANCE ASSIGNMENTS FOR Cd-GAL4 AT pH 7 AND 25 °C<sup>a</sup>

	<sup>15</sup> N	HN	Hα	Hβ	Other	
					<sup>1</sup> H	<sup>15</sup> N
Ser <sup>6</sup>	120.0 <sup>b</sup>	8.35	4.45	3.82,3.88		
Ile <sup>7</sup>	123.7	8.03	4.17	1.85	γ1 1.41,1.15; γ2 0.87; δ 0.78	
Glu <sup>8</sup>	126.0	8.50 <sup>b</sup>	4.31	1.87,2.04	γ 2.22,2.26	
Gln <sup>9</sup>	122.9	8.37	4.43	2.03,2.18	γ 2.49; ε 6.91,7.57	Nε 114.4
Ala <sup>10</sup>	123.6	8.17	4.77	1.52		
Cys <sup>11</sup>	123.9	8.93	4.19	2.98 <i>S</i> ,2.12 <i>R</i>		
Asp <sup>12</sup>	120.6	9.12	4.12	2.60		
Ile <sup>13</sup>	122.0	7.84	3.76	1.77	γ1 0.99,1.53; γ2 0.74; δ 0.68	
Cys <sup>14</sup>	124.8	7.74	3.79	3.31 <i>R</i> ,2.76 <i>S</i>		
Arg <sup>15</sup>	120.0	8.48	4.09	1.80,1.90	γ 1.54; δ 3.16,3.31; ε 7.28	
Leu <sup>16</sup>	122.7	7.84	4.06	1.78,1.70	γ 1.62; δ 0.83,0.93	
Lys <sup>17</sup>	117.7	7.98	4.12	1.91,1.53	γ 1.28,1.36; δ 1.30,1.48; ε 2.40,2.50	
Lys <sup>18</sup>	118.5	7.68	3.88	2.11,1.85	γ 1.33; δ 1.66,1.71; ε 3.03	
Leu <sup>19</sup>	120.7	8.48	4.65	1.82,1.52	γ 1.57; δ1 <i>S</i> 1.01; δ2 <i>R</i> 0.87	
Lys <sup>20</sup>	122.7	8.34	4.31	1.77,1.85	γ 1.47,1.30; δ 1.68; Hε 3.01	
Cys <sup>21</sup>	133.8	8.78	4.70	2.90		
Ser <sup>22</sup>	127.2	8.93	4.50	4.33 <i>S</i> ,3.94 <i>R</i>		
Lys <sup>23</sup>	120.9	9.62	4.51	1.93	γ 1.34,1.44; δ 1.57; ε 2.87,2.93	
Glu <sup>24</sup>	119.8	7.87	4.04	2.02 <i>R</i> ,1.92 <i>S</i>	γ 2.38,2.23	
Lys <sup>25</sup>	119.9	8.32	4.48	1.53 <i>R</i> ,1.68 <i>S</i>	γ 1.14,1.24; δ 1.24,1.19; ε 2.32,1.93	
Pro <sup>26</sup>	<sup>c</sup>	–	4.42	2.48 <i>S</i> ,2.22 <i>R</i>	γ 2.05 <i>R</i> ,1.87 <i>S</i> ; δ 3.45 <i>R</i> ,3.77 <i>S</i>	
Lys <sup>27</sup>	120.6	7.73	5.63	1.61	γ 1.43,1.52; δ 1.43,1.52; ε 3.03	
Cys <sup>28</sup>	126.2	9.36	4.83	3.59 <i>S</i> ,3.78 <i>R</i>		
Ala <sup>29</sup>	123.3	8.13	3.97	1.48		
Lys <sup>30</sup>	121.4	8.13	3.96	1.94	γ 1.30,1.47; δ 1.68; ε 3.05,2.95	
Cys <sup>31</sup>	124.6	7.85	3.99	3.36 <i>R</i> ,2.80 <i>S</i>		
Leu <sup>32</sup>	121.4	8.40	3.99	1.55 <i>S</i> ,1.66 <i>R</i>	γ 1.52; δ 0.87	
Lys <sup>33</sup>	119.9	7.77	3.88	1.65 <i>R</i> ,1.78 <i>S</i>	γ 1.30,1.55; ε 2.90	
Asn <sup>34</sup>	114.5	6.97	4.18	0.62 <i>S</i> ,1.14 <i>R</i>	δ 6.95,6.11	Nδ 115.8
Asn <sup>35</sup>	118.0	7.51	4.37	3.16,2.68	δ 7.49,6.77	Nδ 113.7
Trp <sup>36</sup>	120.7	8.42	5.19	3.47 <i>R</i> ,3.17 <i>S</i>	ε1 10.02; δ1 6.98; ζ2 7.38 η2 7.04; ζ3 6.82; ε3 8.12 γ 2.15,2.24	Nε1 130.0
Glu <sup>37</sup>	123.7	8.64	4.28	1.91 <i>R</i> ,1.96 <i>S</i>		
Cys <sup>38</sup>	132.5	8.12	4.28	3.07 <i>R</i> ,2.65 <i>S</i>		
Arg <sup>39</sup>	131.7	7.83	4.70	1.70,1.72	γ 1.51,1.58; δ 3.14,3.21	
Tyr <sup>40</sup>	125.3	8.92	4.71	2.80	δ 6.93; ε 6.88	
Ser <sup>41</sup>	123.2	9.17	4.72	3.92,3.84		
Pro <sup>42</sup>	<sup>c</sup>	–	4.55	2.29,2.01	γ 1.93; δ 3.81,3.73	
Lys <sup>43</sup>	123.8	8.51	4.31	1.80	γ 1.40; δ 1.80; ε 3.00	

<sup>a</sup> <sup>1</sup>H chemical shifts are referenced to trimethylsilylpropionate (TSP) at 0 ppm. <sup>15</sup>N chemical shifts are referenced to external <sup>15</sup>NH<sub>4</sub>Cl (2.9 M in 1 M HCl at 20 °C) at 24.93 ± 0.05 ppm. *R* and *S* refer to the pro-*R* and pro-*S* configurations, respectively.

<sup>b</sup> Tentative assignment.

<sup>c</sup> Not determined.

the ring resonances for the unique tryptophan (residue 36) and the unique tyrosine (residue 40) of the protein from a TOCSY spectrum. The ring resonances were connected to the  $\beta$  protons using a NOESY spectrum in  $D_2O$ , and the  $\alpha$  and backbone NH protons were identified from a TOCSY spectrum in  $H_2O$ . Spin systems for other residues were identified using TOCSY and DQF-COSY spectra collected in  $H_2O$ . The residues were connected via NOESY connectivities following standard two-dimensional methods (Wüthrich, 1986). The  $^1H$  resonance assignments were confirmed in the 3D NOESY-HSQC spectrum. Stereospecific assignment for the  $\beta$  methylene protons and  $\chi^1$  torsion angles were obtained by consideration of  $^3J(H\alpha, H\beta)$ ,  $NOE(H\alpha, H\beta)$ ,  $NOE(HN, H\beta)$ , and  $^3J(^{15}N, H\beta)$  (Bystrov, 1976; Montelione et al., 1989; Baleja et al., 1992). Additional stereospecific assignments were obtained for the methyl groups of Leu<sup>19</sup> and the  $\gamma$  and  $\delta$  protons of Pro<sup>26</sup> by comparing the quality and final energies of the structures having the two possible chiralities during initial structure calculations. The  $^1H$  and  $^{15}N$  NMR resonance assignments are shown in Table 1. The  $^1H$  resonance assignments for cadmium-GAL4 were published previously (Pan and Coleman, 1991), and extensive corrections to these assignments have been outlined, but not given in detail (Gardner et al., 1991).

NOE intensities were converted to distances as described previously (Baleja et al., 1992). Liganding of the cadmiums was fixed by using distances of  $2.5 \pm 0.05$  Å for Cd to liganding cysteinyl sulfur and  $3.5 \pm 0.25$  Å to the  $\beta$  carbon of the cysteine. Sulfurs liganding the same cadmium ion were constrained to  $4.0 \pm 0.4$  Å, and sulfurs not liganding the same cadmium were forced to be at least 5.5 Å away from the liganding ones. The  $\phi$  torsion angles were derived from  $^3J(NH, H\alpha)$ , measured from observed line splitting of NH resonances from 1D spectra extracted from 2D data (Szyperski et al., 1992). Similarly,  $\chi^1$  torsion angles resulted from the measurement of  $J(\alpha, \beta)$  and

from determining the  $\beta$  proton pro-chirality. A total of 757 distance restraints comprised 92 intraresidue, 221 sequential, 196 medium-range, and 248 long-range restraints. The set of distance restraints and 45 torsion angles were used to calculate 25 structures, 24 of which converged, using previously published methods (Freedman et al., 1995).

The rms deviation to the average structure was  $0.4 \pm 0.05$  Å for backbone atoms, and  $0.9 \pm 0.1$  Å for all heavy atoms (Fig. 2). The coordinates have been deposited with the Protein Data Bank, Brookhaven National Laboratories (entry 1aw6). As a consequence of an additional 57 distance restraints and 14 prochiral assignments, these structures are better refined than in our earlier description (previously the heavy atom rms deviation was  $1.3 \pm 0.2$  Å), although the overall fold of the protein has not changed appreciably. The internal twofold symmetry of the structure has been noted (Baleja et al., 1992), with the backbone atoms of residues 10–22 showing an rms deviation of  $1.3 \pm 0.2$  Å when superimposed on residues 27–39; now the rms deviation is  $0.8 \pm 0.1$  Å. In our earlier study, superimposition with the DNA-bound protein crystallographic structure showed an rms deviation of  $1.1 \pm 0.1$  Å (Baleja et al., 1992). The rms deviation of the refined NMR structures to the X-ray structure is now  $1.0 \pm 0.1$  Å (Fig. 2), and shows preservation of the conformation of the DNA recognition module. The well-determined backbone dihedral angles and side-chain  $\chi^1$  angles are within  $30^\circ$  of those derived crystallographically at 2.7 Å resolution (PDB file name 1d66), reflecting the stability of the bimetal–thiolate cluster, whose conformation does not change appreciably upon binding DNA.

Recently a Karplus-type curve ( $^3J = A \cos^2\phi + B \cos\phi + C$ ) was derived for vicinal  $^3J(^{113}Cd, ^1H\beta)$  coupling constants from the cadmium-substituted protein of rubredoxin and metallothionein (Zerbe et al., 1994), where  $A = 36$ ,  $B = -13$ , and  $C = 1$  Hz. The  $^3J(^{113}Cd, ^1H)$  values for GAL4 were

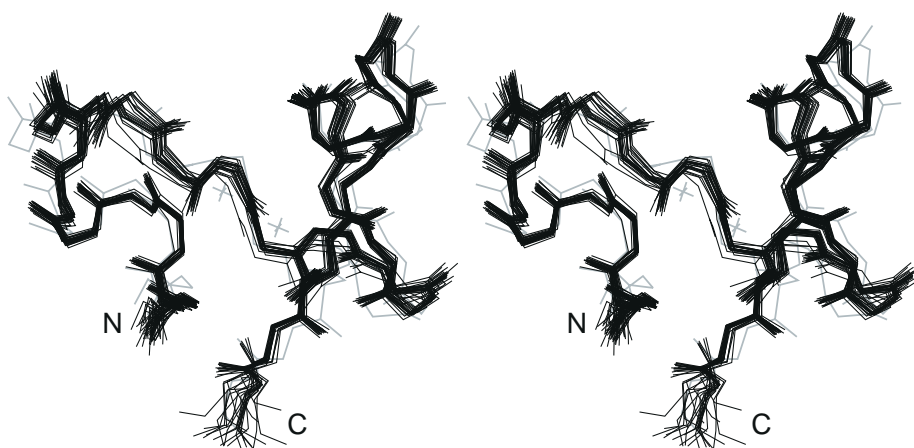


Fig. 2. Stereoview of 24 refined NMR solution structures of GAL4. The backbone atoms are shown superimposed to the crystallographic model (dotted line) by Marmorstein et al. (1992). The rms deviation is  $1.0 \pm 0.1$  Å.

TABLE 2  
CYSTEINE  $^3J(^{113}\text{Cd},^1\text{H})$  COUPLING CONSTANTS AND TORSION ANGLES FOR GAL4<sup>a</sup>

$^{113}\text{Cd},^1\text{H}$	$^3J(^{113}\text{Cd},^1\text{H})$ observed		Torsion angle  (predicted from $J \pm 3$ Hz)		Torsion angle observed	
	<i>R</i>	<i>S</i>	<i>R</i>	<i>S</i>	<i>R</i>	<i>S</i>
Cd <sub>1</sub> ,Cys <sup>11</sup>	11	20	36–50; 107–117	0–29; 121–128	29	148
Cd <sub>1</sub> ,Cys <sup>14</sup>	15	31	27–40; 114–122	135–143	–119	0
Cd <sub>1</sub> ,Cys <sup>21</sup>	55 <sup>b</sup>		nd		–170	–55
Cd <sub>1</sub> ,Cys <sup>28</sup>	2.5	2.5	55–101	55–101	–65	53
Cd <sub>2</sub> ,Cys <sup>11</sup>	2.5	6	55–101	45–62; 97–103	–62	57
Cd <sub>2</sub> ,Cys <sup>28</sup>	10	16	38–51; 105–115	24–38; 115–123	29	147
Cd <sub>2</sub> ,Cys <sup>31</sup>	16	31	24–38; 115–123	135–143	–116	–3
Cd <sub>2</sub> ,Cys <sup>38</sup>	55	18	180 <sup>c</sup>	18–34; 117–126	–171	–55

<sup>a</sup> The absolute values of the coupling constants ( $\pm 3$  Hz) were measured following published procedures (Neuhaus et al., 1984). Sample conditions are given in Table 1. Predicted torsion angles are from a Karplus curve,  $J = A \cos^2\phi + B \cos\phi + C$ , where  $A = 36$ ,  $B = -13$ , and  $C = 1$  (Zerbe et al., 1994). The observed torsion angles are derived from the crystallographic model of GAL4, and agree with those from the NMR solution structure of GAL4 (within  $10^\circ$ ).

<sup>b</sup> Degeneracy of  $\text{H}\beta$  chemical shifts.

<sup>c</sup> The largest coupling constant on the Karplus curve is 50 Hz at  $180^\circ$ .

measured from characteristic heteronuclear coupling patterns observed in  $^1\text{H}\beta\text{R}$ ,  $^1\text{H}\beta\text{S}$  DQF-COSY cross peaks and corresponding cross peaks to the  $\alpha$  proton (Table 2), following established methods (Neuhaus et al., 1984)\*. The cadmiums of observed  $^3J(^{113}\text{Cd},^1\text{H}\beta)$  for the bridging cysteines could be identified by selective decoupling experiments, since the two cadmium resonances are well separated at 669 and 707 ppm (Pan and Coleman, 1990). Given our refined solution structure of Cd-GAL4 and three-bond heteronuclear  $^3J(^{113}\text{Cd},^1\text{H})$  coupling constants for GAL4, we sought to answer the question whether the coupling data on the liganding cysteines fit the published Karplus curve. They do not (Fig. 3). For example, the observed coupling constant for  $\text{H}\beta\text{S}$  of the bridging Cys<sup>11</sup> to cadmium 1 is 20 Hz, suggesting a torsion angle (Cd-S-C $\beta$ -H $\beta$ ) of either near  $15^\circ$  or  $125^\circ$ , which is not close to that observed in the calculated structure ( $148^\circ$ ). A similar discrepancy is observed with  $^3J(^{113}\text{Cd},^1\text{H}\beta\text{R})$  of Cys<sup>11</sup> as well as for the coupling constants and torsion angles for the other, symmetrically related, bridging cysteine (Cys<sup>28</sup>). The discrepancy is not surprising, since the published curve also did not use data from the bridging cysteines of

metallothionein (Zerbe et al., 1994). For example, the published  $^3J(^{113}\text{Cd}(2),^1\text{H}\beta\text{R})$  for the bridging Cys<sup>44</sup> of metallothionein is 12 Hz (Neuhaus et al., 1984; Wagner et al., 1986), whereas the crystal structure shows an angle of  $-21^\circ$  and would predict  $^3J = 20$  Hz. For GAL4, a separate parameterization can reconcile the data ( $A = 19$ ,  $B = -4$ ,  $C = 0$ ,  $R^2 = 0.94$ ), but the same parameterization cannot fit metallothionein. The anomalous curves would result from any factor that alters the hybridization of the atoms, such as variations in the electronic configurations about atoms involved in the torsion angle Cd-S-C $\beta$ -H $\beta$ . For example, the  $^{113}\text{Cd}$ -S-C $\beta$  bond angle varies from  $90^\circ$  to  $110^\circ$  for bridging cysteines, whereas it is rather constant ( $107^\circ \pm 2^\circ$ ) for terminal cysteines. Therefore, because of the constrained geometry for bridging cysteines, the

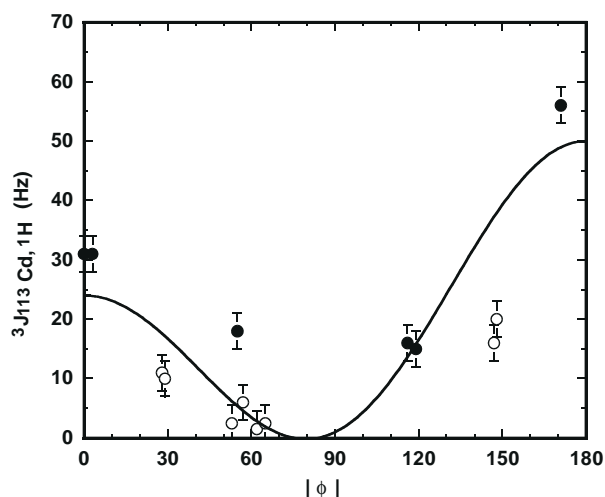


Fig. 3. Plot of the observed  $^3J(^{113}\text{Cd},^1\text{H})$  coupling constants of GAL4 versus the torsion angle. The solid line is derived from the coupling constants of rubredoxin and the non-bridging cysteines of metallothionein (Zerbe et al., 1994). Coupling constants ( $\pm 3$  Hz) of bridging cysteines of GAL4 are shown by open circles, whereas non-bridging cysteines are shown by closed circles.

\*Only five of the six cysteines could be analyzed in full because the  $\beta$  protons of Cys<sup>21</sup> overlap, and the individual  $^3J(^{113}\text{Cd},^1\text{H}\beta\text{R})$  and  $^3J(^{113}\text{Cd},^1\text{H}\beta\text{S})$  coupling constants could not be distinguished. The coupling constants of the other residues agreed with those previously published (Gardner et al., 1991), except for  $^3J(^{113}\text{Cd},^1\text{H}\beta\text{S})$  of Cys<sup>28</sup>, for which we measured 16 Hz rather than 25 Hz, and for  $^3J(^{113}\text{Cd},^1\text{H}\beta\text{S})$  of Cys<sup>38</sup>, for which we measured 18 Hz rather than 26 Hz. The published analysis for Cys<sup>28</sup> includes  $J_{\alpha\beta}$  couplings of 11 and 10 Hz, which are clearly anomalous, since no  $\chi^1$  angle can give such couplings (Wagner, 1990). Our analysis shows instead that the  $J_{\alpha\beta}$  couplings are similar to the symmetrically related Cys<sup>11</sup> residue (both small, corresponding to a  $\chi^1$  of  $+60^\circ$ ), and therefore we believe our  $^3J(^{113}\text{Cd},^1\text{H}\beta\text{S})$  to be more accurate. Likewise, our  $^3J(^{113}\text{Cd},^1\text{H}\beta\text{R})$  for Cys<sup>28</sup> is more accurate since the published analysis includes an anomalous  $J_{\beta\beta}$  of 22 Hz, whereas we obtain the typical 14 Hz (Neuhaus et al., 1984).

Karplus curve of Fig. 3 cannot be used to derive torsion angles accurately from  $^3J(^{113}\text{Cd},\text{H}\beta)$ .

The terminal cysteines of GAL4 then might be expected to follow the curve as expected for metallothionein and rubredoxin. In GAL4, the torsion angle between  $^{113}\text{Cd},\text{H}\beta\text{S}$  of Cys<sup>38</sup> is  $-55^\circ$ , for which the published Karplus curve would predict a coupling of less than 5 Hz. However, the measured  $^3J$  coupling is about 18 Hz. In fact, few of the  $^3J(^{113}\text{Cd},\text{H}\beta)$  couplings for the non-bridging cysteines of GAL4 can be fit using the curve derived from rubredoxin and metallothionein (Fig. 3). Again, the curve could be re-parameterized for GAL4 (with  $A=32$ ,  $B=-12$ ,  $C=10$ ,  $R^2=0.90$ ), but such a re-parameterization clearly undermines the general use of a Karplus curve for torsion angle determination of liganding cysteines in cadmium-substituted proteins. Even in rubredoxin, an unusually large  $^3J(^{113}\text{Cd},\text{H}\beta)$  of 74 Hz for one of the cysteines was clearly outside the expected range (Zerbe et al., 1994).

The differences in parameterization between bridging and non-bridging cysteines of GAL4 are unlikely to arise from measurement errors in either the structures or the measured coupling constants. All Cd-S-C $\beta$ -H $\beta$  torsion angles seen in our NMR structures agree within  $10^\circ$  to those of the crystallographically determined structure (Marmorstein et al., 1992). Likewise, we have independently measured the  $^3J(^{113}\text{Cd},\text{H}\beta)$  couplings, which mostly agree with a set previously published (Gardner et al., 1991).

Similar to the terminal cysteines of GAL4, the cysteines of rubredoxin (PDB entry 1rdg), and the terminal cysteines of metallothionein (PDB file name 4mt2), have no unusual features with respect to their bond lengths, angles, or stereochemistry and, like GAL4, several of the sulfurs of the liganding cysteines participate in hydrogen bonding. What is unusual for GAL4, however, is the double cysteine bridging between cadmium ions coupled with acceptance of hydrogen bonds by the cysteinyl sulfurs (Gregoret et al., 1991; Kraulis et al., 1992; Mau et al., 1992). Partially driven by hydrogen bonding, GAL4 adjusts angles about the S and C $\beta$  atoms (between  $95^\circ$  and  $130^\circ$ ), avoids significant steric clashes between atoms in the metal cluster and contains Cd-S-C $\beta$ -H $\beta$  torsion angles in the range between  $0^\circ$  and  $20^\circ$  and between  $100^\circ$  and  $140^\circ$ , which normally appear disfavored from steric hindrance arguments (Zerbe et al., 1994). We speculate that alterations in electron cloud polarization distort the coupling constants otherwise expected for the torsion angle (Harris, 1983; Zerbe et al., 1994). Our analysis of GAL4 has not defined a single structural parameter or multiple parameters that can predict the anomalous coupling constants.

We conclude that the structural parameters that correlate to  $^3J(^{113}\text{Cd},\text{H}\beta)$  are complex. Although  $^3J(^{113}\text{Cd},\text{H}\beta)$  may show a Karplus-type relationship for some cysteine

residues of some proteins, there appear to be exceptions. In GAL4 the unusual constraints imposed by the bimetal-thiolate cluster result in poor correlation between  $^3J(^{113}\text{Cd},\text{H}\beta)$  and the Karplus-type derived torsion angle.

## Acknowledgements

This work was supported by NIH grants GM47467 (G.W.) and AI38001 (J.D.B.). J.D.B. acknowledges the support of the Medical Research Council of Canada and the Alberta Heritage Foundation for Medical Research. We thank Ted Mau for sample preparation, Dr. Ronen Marmorstein for coordinates of the protein-DNA complex, and Karen Zhang for assistance with cross-peak intensity measurements.

## References

- Baleja, J.D., Marmorstein, R., Harrison, S.C. and Wagner, G. (1992) *Nature*, **356**, 450–453.
- Bystrov, V.F. (1976) *Prog. NMR Spectrosc.*, **10**, 41–81.
- Freedman, S.J., Furie, B.C., Furie, C. and Baleja, J.D. (1995) *Biochemistry*, **34**, 12126–12137.
- Gardner, K.H., Pan, T., Narula, S., Rivera, E. and Coleman, J.E. (1991) *Biochemistry*, **30**, 11292–11302.
- Gregoret, L.M., Rader, S.D., Fletterick, R.J. and Cohen, F.E. (1991) *Proteins Struct. Funct. Genet.*, **9**, 99–107.
- Harris, R.K. (1983) In *Nuclear Magnetic Resonance Spectroscopy*, Pitman, London, U.K., pp. 211–227.
- Johnston, M. (1987) *Micro. Rev.*, **51**, 458–476.
- Kraulis, P.J., Raine, A.R.C., Gadhavi, P.L. and Laue, E.D. (1992) *Nature*, **356**, 448–450.
- Lefèvre, J.-F., Dayie, K.T., Peng, J.W. and Wagner, G. (1996) *Biochemistry*, **35**, 2674–2686.
- Marmorstein, R., Carey, M., Ptashne, M. and Harrison, S.C. (1992) *Nature*, **356**, 408–414.
- Mau, T., Baleja, J.D. and Wagner, G.W. (1992) *Protein Sci.*, **1**, 1403–1412.
- Montelione, G.T., Winkler, M.E., Rauenbuehler, P. and Wagner, G. (1989) *J. Magn. Reson.*, **82**, 198–204.
- Neuhaus, D., Wagner, G., Vašák, M., Kägi, J.H.R. and Wüthrich, K. (1984) *Eur. J. Biochem.*, **143**, 659–667.
- Pan, T. and Coleman, J.E. (1989) *Proc. Natl. Acad. Sci. USA*, **86**, 3145–3149.
- Pan, T. and Coleman, J.E. (1990) *Biochemistry*, **29**, 3023–3029.
- Pan, T. and Coleman, J.E. (1991) *Biochemistry*, **30**, 4212–4222.
- Povey, J.F., Diakun, G.P., Garner, C.D., Wilson, S.P. and Laue, E.D. (1990) *FEBS Lett.*, **266**, 142–146.
- Shirakawa, M., Fairbrother, W.J., Serikawa, Y., Ohkubo, T., Kyo-goku, Y. and Wright, P.E. (1993) *Biochemistry*, **32**, 2144–2153.
- Szyperski, T., Güntert, P., Otting, G. and Wüthrich, K. (1992) *J. Magn. Reson.*, **99**, 552–560.
- Wagner, G., Neuhaus, D., Wörgötter, E., Vašák, M., Kägi, J.H.R. and Wüthrich, K. (1986) *Eur. J. Biochem.*, **157**, 275–289.
- Wagner, G. (1990) *Prog. NMR Spectrosc.*, **22**, 101–139.
- Wüthrich, K. (1986) *NMR of Proteins and Nucleic Acids*, Wiley, New York, NY, U.S.A.
- Zerbe, O., Pountney, D.L., von Philipsborn, W. and Vašák, M. (1994) *J. Am. Chem. Soc.*, **116**, 377–378.